SCIENTIFIC REPORTS

OPEN

SUBJECT AREAS:
BIOPHYSICAL CHEMISTRY
ANTIBODY THERAPY

Received
12 September 2014

Accepted
9 December 2014

Published
15 January 2015

Correspondence and requests for materials should be addressed to J.C.W. (jcwilliams@coh.org)

Development of a High Affinity, Non-covalent Biologic to Add Functionality to Fabs

Kendra N. Avery, Cindy Zer, Krzysztof P. Bzymek & John C. Williams

Department of Molecular Medicine, Beckman Research Institute at City of Hope 1710 Flower St, Duarte CA 91010.

Functionalization of monoclonal antibodies (mAbs) requires chemical derivatization and/or genetic manipulation. Inherent in these methods are challenges with protein heterogeneity, stability and solubility. Such perturbations could potentially be avoided by using a high affinity, non-covalent intermediate to bridge the desired functionality to a stable mAb. Recently, we engineered a binding site for a peptide named "meditope" within the Fab of trastuzumab. Proximity of the meditope site to that of protein L suggested an opportunity to enhance the meditope's moderate affinity. Joined by a peptide linker, the meditope-protein L construct has a $K_D \sim 180$ pM - a 7000-fold increase in affinity. The construct is highly specific to the engineered trastuzumab, as demonstrated by flow cytometry. Moreover, the fusion of a bulky GFP to this construct did not affect the association with cell surface antigens. Collectively, these data indicate this specific, high affinity construct can be developed to rapidly add new functionality to mAbs.

Antibodies, with their serum stability and antigen specificity, are uniquely suitable carriers of imaging agents, cytotoxins and immunomodulatory molecules to specific disease sites in the body[1–3]. The recent United States Food and Drug Administration approval of trastuzumab emtansine and brentuximab vedotin to treat HER2+ breast cancer and refractory Hodgkin's lymphoma, respectively, has provided support to the field of antibody-drug conjugates. Likewise, the use of radionuclide-conjugated mAbs to image diseased tissues and metastases by positron emission tomography is showing promising results and likely will become an important clinical tool[4].

Despite the success of these mAb conjugates, limitations in the current approach of creating targeted therapeutics are hindering the full actualization of their clinical application. Invariably, the small molecule drug payload or radionuclide chelator must be covalently attached to surface-exposed lysines, cysteines or other engineered amino acids on a mAb[5–7]. Because of the limited conjugation site selectivity and inherent inefficiencies in the coupling chemistries, heterogeneous mixtures of mAb conjugates are often produced. The components of these mixtures have differing pharmacodynamic and pharmacokinetic properties, further complicating the development of functionalized mAb-based therapeutics.

Based on our recent studies, we propose a stable, non-covalent, site-specific method for attaching drugs or imaging agents to therapeutic mAbs as an alternative to covalent conjugation. Previously, we defined the binding site of a small peptide we called "meditope" within the Fab arm of cetuximab, a chimeric anti-EGFR mAb used to treat colorectal cancer[8]. The affinity is moderate ($K_D = \sim 1$ μM), but meditope does not interfere with antigen binding. This meditope binding site, absent in human mAbs, can be readily grafted through a small number of mutations without notably altering the stability or activity of the mAb as exemplified by our "meditope-enabling" of trastuzumab, a humanized, anti-HER2 mAb approved to treat breast cancer[8]. Upon solving the atomic structure of the "meditope-enabled" trastuzumab (memAb trastuzumab) Fab bound to meditope and single Fab binding domains of protein L and protein A (included to aid crystallization), we observed that the termini of meditope and protein L were in close proximity (Figure 1A). Although the affinities of either meditope or protein L are insufficient to replace a covalent interaction, we hypothesized that fusion of meditope to protein L through an appropriate linker would produce a high-affinity, high-specificity tether with controlled stoichiometry to functionalize mAbs for a host of mAb-based applications[9].

Results

The distance between the C-terminus of meditope and N-terminus of protein L is 15.7 Å (Figure 1A)[8], and we estimated that a linker composed of three to nine residues would permit the binding of both moieties simulta-

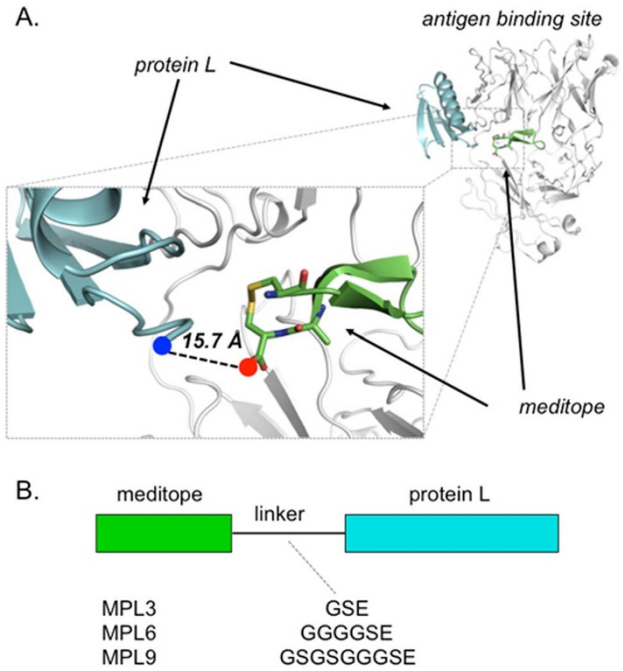

Figure 1 | Meditope and protein L binding to memAb trastuzumab. (A) Ribbon representation of meditope, protein L and memAb Fab with estimated linker distance (4IOI). (B) Schematic of the MPL constructs and the composition of the various linkers.

neously. Therefore, we designed meditope-protein L (MPL) variants that had three-, six-, or nine- glycine and serine linkers (Figure 1B), as well as a zero length linker as a baseline. We measured the binding constants of each variant to memAb trastuzumab by surface plasmon resonance (SPR). All MPL linker variants bound to memAb trastuzumab with improved affinity as compared to the individual components; the six-amino acid linker was the most optimal (Table 1, Figure S1). The calculated binding constants of the MPL variants with different linker lengths were, in pM, K_D = 170,000 ± 120,000 (zero), 870 ± 500 (three), 180 ± 40 (six) and 280 ± 90 (nine) (Table 1 and Figure S2). The zero length construct may still be able to bind in a bivalent fashion due to the flexibility of the N-terminus of protein L or perhaps a residue in the meditope is in position to make a productive bond with the Fab.

To confirm that the high affinity binding of MPL6 was due to multivalency, we measured the binding affinities of the individual components and MPL variants that had either F3A and R8A mutations to abolish meditope binding, or Y51W and L55H mutations to weaken protein L binding to memAb trastuzumab[8,10]. The dissociation constant of meditope was K_D = 1.3 ± 0.2 μM while that of protein L was K_D = 1.2 ± 0.7 μM (Figure S1B–C). The meditope-mutated MPL6$^{F3A/R8A}$ variant had significantly reduced affinity for the Fab (K_D = 450 ± 240 nM) (Figure S1D). Similarly, the protein L-mutated MPL6$^{Y51W/L55H}$ variant showed significantly reduced affinity (K_D = 180 ± 120 nM) (Figure S1E), and the SPR traces no longer fit well with a 1 : 1 binding model, suggesting that multiple modes of interaction may be present, possibly due to the incomplete disruption of protein L binding by the point mutations (Table 1, Figure S1).

Based on energy additivity (i.e., $\Delta G_{total} = \Delta G_1 + \Delta G_2 - \Delta G_{interaction}$), the anticipated binding constant of the bivalent MPL construct, assuming an ideal linker ($\Delta G_{interaction} = 0$) should be $K_{D1} * K_{D2}/1\ M = 1.3 \times 10^{-6}\ M * 1.2 \times 10^{-6}\ M/1\ M = 1.6 \times 10^{-12}$ M, or 1.6 pM[11,12]. We expected entropic penalties due to the loss of rotational and translational degrees of freedom[11–13], but also note that the linker could interact with the protein to produce a favorable interaction[14]. These potential penalties or gains are captured by the $\Delta G_{interaction}$ term. The resulting gain in affinity for the MPL6 variant (K_D = 180 ± 40 pM) was more than 7,000-fold greater than for the meditope alone and within two orders of magnitude of an "ideal" linker. To the best of our knowledge, this is the highest affinity ligand that binds specifically to a Fab framework.

We also explored the effects of rigidifying the linker to decrease conformational entropy by the introduction of proline residues to the linker[13,15–18]. We made MPL3 variants with linkers composed of PSE, PPE and PPP and tested each by SPR analysis for binding to memAb trastuzumab. We found modest improvement in binding affinities for linkers PPE (410 ± 180 pM) and PPP (650 ± 200 pM) as compared to the original GSE linker (870 ± 500 pM) but a moderate decrease for linker PSE (1300 ± 1200 pM) (Figure 2, Table 1, Figure S3). Next, we substituted the favorable MPL6 flexible linker GGGGSE with different numbers of proline residues to make three additional MPL6 variants with PPPPPP, PPPGPP and GGPGSE linkers. The affinity of the all proline linker was ~28 fold weaker (K_D = 5100 ± 3100 pM) than the original MPL6, and the data did not fit well with a 1 : 1 binding model. The PPPGPP variant was slightly better (K_D = 1100 ± 500 pM), and the most flexible, least substituted GGPGSE variant was very similar to the optimal MPL6 (K_D = 180 ± 20 pM). None of the proline-containing linkers were an improvement over the original MPL6 (Figure 2, Table 1, Figure S3), indicating, albeit from a limited set of data, that conformational entropy, in this particular system, was not a large contributing factor[13].

To determine how MPL6 binding affects the affinity of the Fab to antigen, we measured the binding affinity of memAb trastuzumab Fab to immobilized HER2 in the presence or absence of MPL6 (Figure 3A–B; Figure S4A–B). The affinity of memAb trastuzumab Fab to HER2 alone was similar to when saturating concentrations of

Table 1 | Summary of binding affinity and kinetic parameter measurements of MPL variants to meditope enabled trastuzumab by SPR

	k_a (M^{-1} s^{-1})	k_d (s^{-1})	Dissociation constant, K_D (nM)
meditope	1.2 +/− 0.13 × 10^4	1.7 +/− 0.01 × 10^{-2}	1300 +/− 150
protein L	6.4 +/− 1.8 × 10^4	5.9 +/− 2.3 × 10^{-2}	1200 +/− 720
MPL6 (GGGGSE)	7.9 +/− 3.9 × 10^5	2.0 +/− 1.8 × 10^{-4}	0.19 +/− 0.038
MPL6 F3A R8A	7.3 +/− 1.1 × 10^4	3.1 +/− 1.3 × 10^{-2}	450 +/− 240
MPL6 Y51W L55H	1.1 +/− 0.76 ×10^5	2.4 +/− 2.6 × 10^{-2}	180 +/− 120*
MPL3 (GSE)	4.2 +/− 2.7 × 10^5	2.7 +/− 0.92 × 10^{-4}	0.87 +/− 0.50
MPL9 (GSGSGGGSE)	4.6 +/− 0.18 × 10^5	1.3 +/− 0.41 × 10^{-4}	0.28 +/− 0.088
MPL no linker	1.6 +/− 1.6 × 10^5	1.4 +/− 0.68 × 10^{-2}	170 +/− 120
MPL3 (PSE)	3.2 +/− 1.7 × 10^5	2.9 +/− 1.4 × 10^{-4}	1.3 +/− 1.2
MPL3 (PPE)	9.6 +/− 7.0 × 10^5	3.8 +/− 0.42 × 10^{-4}	0.41 +/− 0.18
MPL3 (PPP)	4.1 +/− 0.52 × 10^5	2.7 +/− 1.2 × 10^{-4}	0.65 +/− 0.20
MPL6 6 Pro (PPPPPP)	2.0 +/− 0.84 × 10^5	1.7 +/− 0.56 × 10^{-3}	5.1 +/− 3.2*

*indicates deviation in the fit from a 1 : 1 binding model.

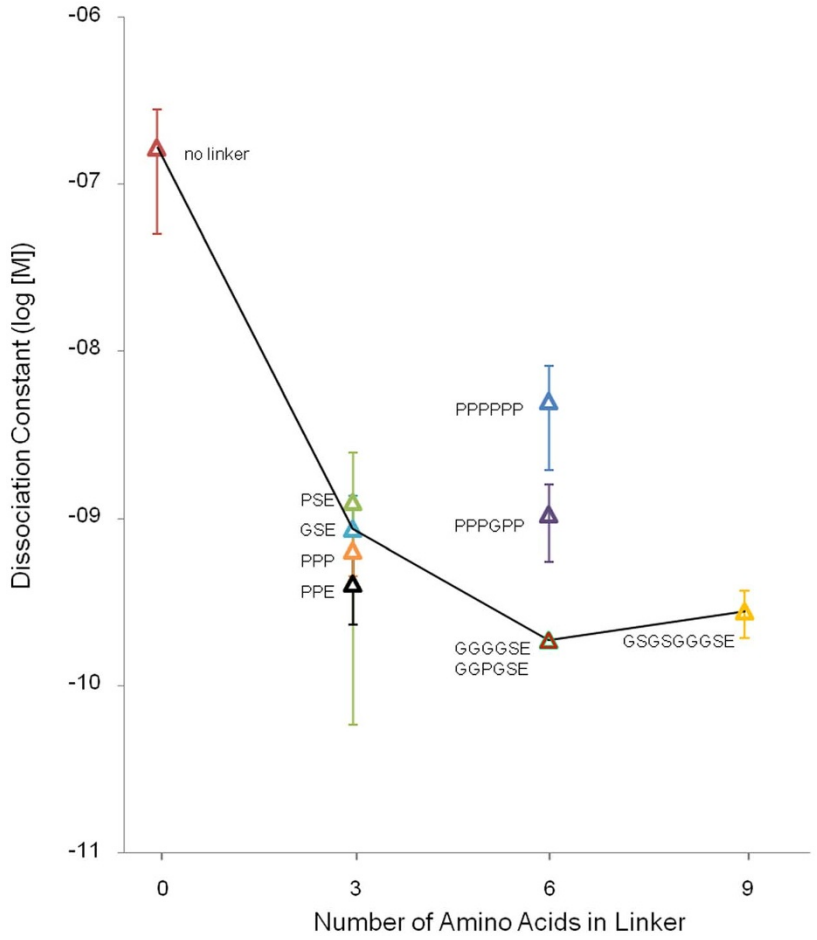

Figure 2 | Graph correlating MPL linker length and composition with dissociation constants for binding to memAb trastuzumab.

MPL6 were present, K_D = 190 ± 98 pM and 130 ± 40 pM, respectively and the on- and off- rates were also similar (Table S1).

Armed with this small (~8 kDa), high affinity and non-antigen binding interfering Fab framework ligand, we set out, as proof-of-concept, to establish that the MPL-memAb trastuzumab interaction could be used to add functionality to memAbs for *in vitro* imaging of cancer cells. We mixed Alexa Fluor 647-labeled MPL6 with Alexa Fluor 488-labeled memAb trastuzumab and incubated the mixture with HER2 over-expressing SKBR3 breast cancer cells. FACS showed that the cells were simultaneously labeled by both MPL6 and memAb trastuzumab (Figure 4A). To mimic a pre-targeted imaging strategy[1], we incubated memAb trastuzumab and MPL6 sequentially with SKBR3 cells and washed the cells extensively between treatments. The levels of staining of the SKBR3 cells by both ligands were indistinguishable between the co- and sequential incubation procedures, indicating robust binding of MPL to memAb trastuzumab (Figure 4B). Although MPL6 can bind to the unmodified parental trastuzumab through protein L (Figure S5), the affinity was far weaker than for memAb trastuzumab; thus MPL6 rapidly dissociated from parental trastuzumab during standard FACS washing procedures.

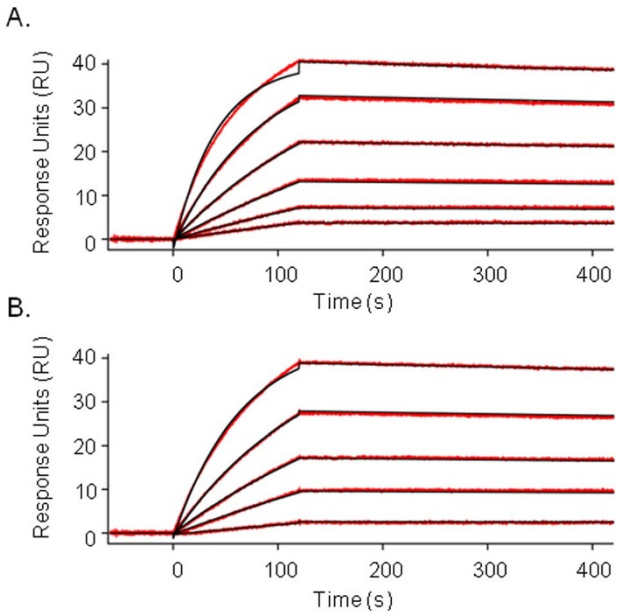

Figure 3 | Representative SPR sensograms showing the binding interaction of (A) memAb Fab with immobilized HER2 and (B) memAb Fab pre-incubated with excess MPL6 with immobilized HER2.

The FACS experiments proved the feasibility of displacing the conjugation of small fluorescent dyes from the mAb itself to MPL for imaging purposes. To demonstrate the versatility of MPL6 to provide additional functionality to memAbs, we fused green fluorescent protein (GFP), a comparatively bulky addition, to the C-terminus of MPL6 through a short flexible linker. SPR studies confirmed that the fusion of GFP did not prohibit the binding of MPL6 to memAb trastuzumab, nor did MPL6-GFP mixed with memAb trastuzumab prevent antigen binding, though we did observe a difference in the binding affinities (~7 fold lower for memAb and ~3 fold lower for the complex to antigen), which appeared to be predominantly due to changes in the on-rates (Figure S4 C–D, Table S1). Furthermore, fluorescence microscopy

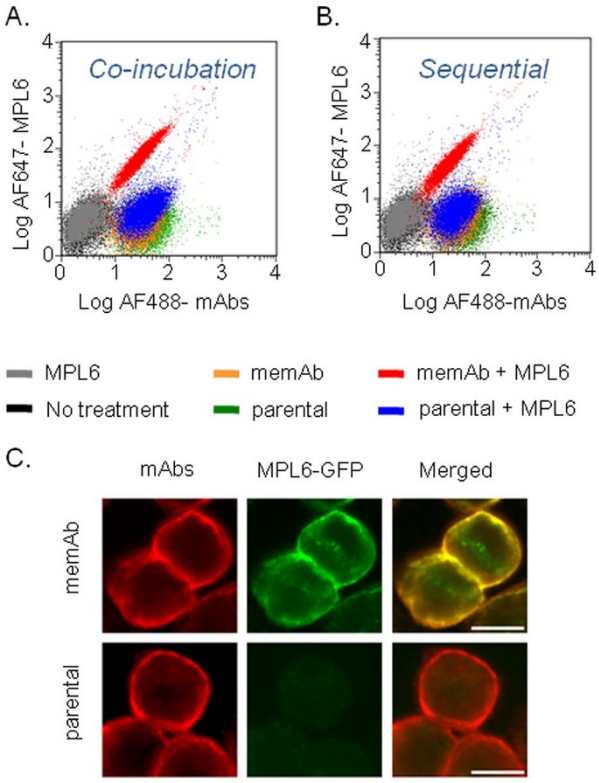

Figure 4 | Utility of MPL6 for imaging. FACS analyses of SKBR3 cells treated (A) with co-incubation or (B) sequentially with parental or memAb trastuzumab and MPL6. (C) Fluorescent microscopy images of SKBR3 cells treated with parental or memAb trastuzumab and MPL6-GFP (scale bar = 10 μm).

indicated the addition of GFP did not affect binding of the complex to cell-associated antigen (Figure 4C).

Discussion

Collectively, the design and subsequent engineering of the meditope-protein L construct indicated that it is possible to create a high affinity ligand that binds to the meditope-enabled Fab framework, does not affect antigen binding, and can be functionalized chemically or through the fusion of a larger protein. We chose to fuse GFP to MPL6 for proof-of-concept, but it is possible to envision a host of biologics that could be fused to MPL6 to image and/or treat disease[19–21]. Furthermore, due to the small size and bacterial production of MPL6, it is straightforward to engineer lysine or cysteine residues within MPL6, and/or non-natural amino acids for site specific chemical conjugation[22]. Additional efforts are needed to make non-covalent functionalization of mAbs a general principle including grafting of the meditope-binding site of the parental mAb; however, these initial studies indicate that it is possible to develop a "plug-and-play" system where a single mAb (meditope-enabled) could be rapidly linked to a wide array of "widgets" through a high affinity intermediate (MPL), leading to a homogeneous population of functionalized mAbs. Future work will involve the de-immunization of protein L using methods that have been successful for a variety of bacterial and plant derived immunotoxins and affibodies. Moreover, these efforts will also focus on improving the selectivity of MPL for memAbs over endogenous mAbs[23–25].

Methods

Protein expression/purification. MPL mutants were expressed as His6-SMT3 fusions in BL21 (DE3) *E. coli*, purified by Ni-NTA (Thermo Scientific HisPur) affinity chromatography, cleaved by ULP1-His6 and separated by reverse Ni-NTA, followed by gel filtration chromatography on a Superdex G75 preparative column (GE Healthcare). MemAb trastuzumab was expressed and purified as previously described[8].

Surface Plasmon Resonance. Kinetics experiments were performed on a GE Biacore T100 using Series S CM5 sensor chips at flow rate of 30 μL/min in HBS-EP+ (GE) at 25°C. Ligands were covalently coupled to the chip surface using standard amine coupling protocols (EDC/NHS chemistry) at density levels suitable for kinetics experiments. Data sets were run in replicate. Kinetic parameters were calculated using BIAEvaluation software.

Analytic Cytometry. SKBR3 cells were maintained in 10% FBS-supplemented DMEM at 37°C and 5% CO_2 humidified atmosphere. Each sample contained 1×10^6 cells that were trypsinized, washed with wash buffer ([WB] 0.3% BSA in PBS) and incubated with 100 μL of 10 nM of either mAb and 50 nM of MPL6 for 30 min on ice. Alternatively, cells were first incubated with either mAb for 15 min, washed with WB, then incubated another 15 min with MPL6 on ice. After incubation, the cells were washed twice with WB and resuspended in WB supplemented with SYTOX® Blue (Invitrogen). FACS was performed on a CyAn™ ADP Analyzer (Beckman Coulter). Data were analyzed with Flowjo software.

Microscopy. SKBR3 cells (5×10^4) were seeded onto cover slips overnight. The culture medium was replaced with 250 μL of medium containing 50 nM AF 555-labeled memAb or parental trastuzumab and 250 nM MPL6-GFP at 37°C for 30 min. The cells were washed twice with pre-warmed PBS, fixed with room temperature 3.7% formaldehyde in PBS, washed twice with room temperature PBS, and mounted with ProLong® Gold Antifade Reagent with DAPI (Invitrogen) onto glass slides. Images were taken with an Olympus I × 81 automated inverted microscope at 64X magnification and processed with Photoshop software.

Please see the supplementary information section for detailed materials and methods.

1. Goldenberg, D. M. *et al.* Pretargeted molecular imaging and radioimmunotherapy. *Theranostics* **2**, 523–540, doi:10.7150/thno.3582 (2012).
2. Scott, A. M., Wolchok, J. D. & Old, L. J. Antibody therapy of cancer. *Nat Rev Cancer* **12**, 278–287, doi:10.1038/nrc3236 (2012).
3. Weiner, L. M., Murray, J. C. & Shuptrine, C. W. Antibody-based immunotherapy of cancer. *Cell* **148**, 1081–1084, doi:10.1016/j.cell.2012.02.034 (2012).
4. Steiner, M. & Neri, D. Antibody-radionuclide conjugates for cancer therapy: historical considerations and new trends. *Clin Cancer Res* **17**, 6406–6416, doi:10.1158/1078-0432.CCR-11-0483 (2011).
5. Sievers, E. L. & Senter, P. D. Antibody-drug conjugates in cancer therapy. *Annual review of medicine* **64**, 15–29, doi:10.1146/annurev-med-050311-201823 (2013).
6. Junutula, J. R. *et al.* Engineered thio-trastuzumab-DM1 conjugate with an improved therapeutic index to target human epidermal growth factor receptor 2-positive breast cancer. *Clin Cancer Res* **16**, 4769–4778, doi:10.1158/1078-0432.CCR-10-0987 (2010).
7. Hamblett, K. J. *et al.* Effects of drug loading on the antitumor activity of a monoclonal antibody drug conjugate. *Clin Cancer Res* **10**, 7063–7070, doi:10.1158/1078-0432.CCR-04-0789 (2004).
8. Donaldson, J. M. *et al.* Identification and grafting of a unique peptide-binding site in the Fab framework of monoclonal antibodies. *Proc Natl Acad Sci U S A* **110**, 17456–17461, doi:10.1073/pnas.1307309110 (2013).
9. Mammen, M., Choi, S. K. & GM, W. Polyvalent interactions in biological systems: Implications for design and use of multivalent ligands and inhibitors. *Angew. Chem. Int. Ed. Eng.* **37**, 2755–2794 (1998).
10. Housden, N. G. *et al.* Observation and characterization of the interaction between a single immunoglobulin binding domain of protein L and two equivalents of human kappa light chains. *J Biol Chem* **279**, 9370–9378, doi:10.1074/jbc.M312938200 (2004).
11. Jencks, W. On the attribution and additivity of binding energies. *Proc Natl Acad Sci U S A* **78**, 4046–4050 (1981).
12. Kane, R. S. Thermodynamics of multivalent interactions: influence of the linker. *Langmuir: the ACS journal of surfaces and colloids* **26**, 8636–8640, doi:10.1021/la9047193 (2010).
13. Mack, E. T. *et al.* Dependence of avidity on linker length for a bivalent ligand-bivalent receptor model system. *J Am Chem Soc* **134**, 333–345, doi:10.1021/ja2073033 (2012).
14. Numata, J., Juneja, A., Diestler, D. J. & Knapp, E. W. Influence of spacer-receptor interactions on the stability of bivalent ligand-receptor complexes. *The journal of physical chemistry. B* **116**, 2595–2604, doi:10.1021/jp211383s (2012).
15. Arora, P. S., Ansari, A. Z., Best, T. P., Ptashne, M. & Dervan, P. B. Design of artificial transcriptional activators with rigid poly-L-proline linkers. *J Am Chem Soc* **124**, 13067–13071 (2002).
16. Mack, E. T., Perez-Castillejos, R., Suo, Z. & Whitesides, G. M. Exact analysis of ligand-induced dimerization of monomeric receptors. *Anal Chem* **80**, 5550–5555 (2008).
17. Kitov, P. I., Shimizu, H., Homans, S. W. & Bundle, D. R. Optimization of tether length in nonglycosidically linked bivalent ligands that target sites 2 and 1 of a Shiga-like toxin. *J Am Chem Soc* **125**, 3284–3294, doi:10.1021/ja0258529 (2003).

18. Merritt, E. A. *et al.* Characterization and crystal structure of a high-affinity pentavalent receptor-binding inhibitor for cholera toxin and E. coli heat-labile enterotoxin. *J Am Chem Soc* **124**, 8818–8824 (2002).
19. LaFleur, D. W. *et al.* Monoclonal antibody therapeutics with up to five specificities: functional enhancement through fusion of target-specific peptides. *MAbs* **5**, 208–218, doi:10.4161/mabs.23043 (2013).
20. Antignani, A. & Fitzgerald, D. Immunotoxins: the role of the toxin. *Toxins* **5**, 1486–1502, doi:10.3390/toxins5081486 (2013).
21. Park, J. I. *et al.* Antitumor therapy mediated by 5-fluorocytosine and a recombinant fusion protein containing TSG-6 hyaluronan binding domain and yeast cytosine deaminase. *Mol Pharm* **6**, 801–812, doi:10.1021/mp800013c (2009).
22. Liu, C. C. & Schultz, P. G. Adding new chemistries to the genetic code. *Annu Rev Biochem* **79**, 413–444, doi:10.1146/annurev.biochem.052308.105824 (2010).
23. Parker, A. S., Choi, Y., Griswold, K. E. & Bailey-Kellogg, C. Structure-guided deimmunization of therapeutic proteins. *J Comput biol.* **20**, 152–165, doi:10.1089/cmb.2012.0251 (2013).
24. Amann, M. *et al.* Antitumor activity of an EpCAM/CD3-bispecific BiTE antibody during long-term treatment of mice in the absence of T-cell anergy and sustained cytokine release. *J Immunother* **32**, 452–464, doi:10.1097/CJI.0b013e3181a1c097 (2009).
25. Herne, N. Method for reducing the immune response to a biologically active protein. Affibody, assignee. Patent US 8642743 B2. 4 Feb. 2014. Print.

Acknowledgments

J.C.W. acknowledges support from the Alicia and John Kruger Gift, Albert Trust, and Grant Number R21 CA135216 from NCI. We also acknowledge the Drug Discovery and Structural Biology Core, supported by Grant Number P30 CA033572 from the NCI. C.Z. acknowledges support from the Gastrointestinal Cancers Program Pilot Grant at City of Hope. We thank current and former members of the Williams laboratory and Dr. Gagandeep Singh for helpful insights and discussions.

Author contributions

K.N.A. designed, generated, purified and characterized all MPL constructs; C.Z. provided reagents, characterized cell binding and imaging experiments; K.P.B. provided experimental advice; J.C.W. designed and supervised the overall project. All authors contributed to the writing, figures and editing of the manuscript.

Additional information

Supplementary information accompanies this paper at http://www.nature.com/scientificreports

Competing financial interests: Dr. Williams is member of the scientific advisory board of Meditope Biosciences, Inc. and owns stock in the company. Drs. Avery, Zer and Bzymek declare no potential conflict of interest.

How to cite this article: Avery, K.N., Zer, C., Bzymek, K.P. & Williams, J.C. Development of a High Affinity, Non-covalent Biologic to Add Functionality to Fabs. *Sci. Rep.* **5**, 7817; DOI:10.1038/srep07817 (2015).

This work is licensed under a Creative Commons Attribution-NonCommercial-NoDerivs 4.0 International License. The images or other third party material in this article are included in the article's Creative Commons license, unless indicated otherwise in the credit line; if the material is not included under the Creative Commons license, users will need to obtain permission from the license holder in order to reproduce the material. To view a copy of this license, visit http://creativecommons.org/licenses/by-nc-nd/4.0/